RESEARCH DEPARTMENT
TECHNICAL REPORT No. 48

A NUMERICAL CASE STUDY OF EAST ASIAN COASTAL CYCLOGENESIS

by

Shou-Jun Chen* and Lorenzo Dell'Osso

*On leave from
Department of Geophysics,
Peking University,
Beijing, China

May 1985

Abstract

The relative importance of latent heat release in East Asian coastal cyclogenesis is investigated by performing numerical experiments with the ECMWF limited area model. The cyclone obtained in the Moist simulation developed in a way similar to that observed, while in the Dry simulation a shallow low appeared when the upper wave trough approached the inverted surface trough situated on the coast, but no further development took place. The baroclinic forcing is only a trigger for the development.

The latent heat release enhanced the vertical circulation at the eastern side of the upper trough and caused the upper frontogenesis. Thus the available potential energy, as well as the conversion from available potential energy to kinetic energy, was increased in the wave domain and this was favourable for the development.

C O N T E N T S

1. INTRODUCTION

In the nineteenth and early twentieth century, the thermal theory of cyclones viewed mid-latitude cyclones as being driven primarily by the release of latent heat in the ascending air (Kutzbach, 1979). In the 1920's, the thermal theory was replaced by the polar-front theory (Bjerknes, 1919); in this the available potential energy provided by the temperature contrast between polar and tropical air (instead of the latent heat release) was considered as the initial energy source for cyclone development, and cyclogenesis was viewed as an instability of the frontal surface of discontinuity. Eliassen (1966) concluded that the instability of a frontal surface may be responsible for only the growth of short, shallow cyclone waves. The development of quasi-geostrophic theory and the theoretical studies of baroclinic instability by Charney (1947) and Eady (1949) lead to the view that baroclinic instability is the dominant process for intense mid-latitude cyclogenesis; the fronts then develop in response to wave amplification. The vertical velocity which is driven by vertical differential vorticity advection and the Laplacian of thermal advection converts eddy available potential energy to eddy kinetic energy, thus causing the development (Holton, 1979).

Since the 1950's, the impact of release of latent heat in cyclone development was again brought to meteorologists' attention (e.g. Aubert, 1957. Danard, 1964). It is in this context that we examine an example of East Asian coastal cyclogenesis.

In winter, the subtropical and polar jet streams merge over the East Asian continent. The confluence of the large scale upper flows causes the development of a few cyclones which can be observed over Mongolia and Northeast China (Staff members, Academia Sinica, 1958). Over the mainland, many cyclonic circulations appear as shallow lows or inverted troughs. But,

if these weak disturbances move off the coast, sometimes they deepen very quickly: a drop of central pressure of more than 20 mb in 24 h is not unusual. The cyclones which develop over the Yellow Sea and the East Sea often cause strong gales; then as they continue to deepen, they move north-eastward and eventually become huge lows over the Aleutian region and form part of the semi-permanent action-centre. Thus the behaviour of coastal cyclones is important for weather forecasting over East Asia as well as understanding the general circulation.

Among the synoptic and numerical studies of North American coastal cyclones, Bosart's work on the major coastal cyclone of 18-19 February 1979, known as the Presidents' Day Cyclone (Bosart, 1981), is especially noteworthy. He pointed out that the treatment of moist diabatic effects in numerical model is very important for achieving an accurate forecast of the rapid development of this cyclone. For East Asian coastal cyclogenesis, an early synoptic study showed that a wide precipitation area occurred over the coast before the cyclone was initiated (Chen, 1954); this suggests the impact of the latent heat release is significant. A numerical case study presented by Hoskins (1980) also showed the role of latent heating in the cyclone development over the Western Pacific, but a detailed analysis was not given. Recently, Chen et al. (1983) performed some numerical experiments for an AMTEX'75 oceanic cyclone which started over the ocean south of Japan (near 125°E,25°N) and developed into an intense extratropical cyclone during the next 24 hours.

It was found that latent heating had a profound impact on the intensity of the storm. Both the numerical studies carried out by Hoskins (1980) and Chen et al. (1983) only concern oceanic cyclones. Therefore in this study we examine the role of latent heat in the development of a coastal cyclone.

The model used in this study is a limited area version of the ECMWF global grid point model (Burridge and Hasler, 1977). It uses σ as vertical coordinate with 15 levels and a horizontal resolution of 1.875° of latitude and longitude. The physics of the model contains large scale latent heating, a modified Kuo's convective parameterization scheme (Kuo, 1974), planetary boundary layer physics, radiation, and the surface fluxes of sensible and latent heat. A more detailed description of the model physics can be found in Tiedtke et al. (1979). The model domain was 15°N-65°N and 70°E-180°E, and the boundary values were obtained from analyses every 12 hours. In the following sections we focus our attention on how the latent heat release influences the behaviour of an East Asian coastal cyclone.

2. SYNOPTIC DESCRIPTION

On 00GMT 28 November 1982, cyclogenesis occurred along the East Asian coast and the initial shallow depression developed into a major deep cyclone in two days. Fig. 1 shows the 500 mb and 1000 mb analyses, from 00GMT 28 November to 00GMT 30 November 1982. At 00GMT, 28 November at 1000 mb, an anticyclonic circulation occupied the southern part of the mainland, with cold air established over eastern China. There was also a weak high over the Western Pacific. An inverted trough was located on the western coast of East Asia and orientated approximately north-south (along 120°E). At 500 mb, the dominant feature over China was a short wave trough along 108°E which extended from Gansu to Sichun province. The lag of the thermal trough behind the pressure trough indicates cold advection along the trough line. As the upper trough approached the surface inverted trough, a cyclone started to form at the tip of the surface trough. This situation was very similar to the cyclone development described by Petterssen (1956).

By 00GMT on 29 November a cyclonic closed centre, with central pressure of 1008 mb formed over the Yellow Sea. The associated fronts became well defined, and formed a warm sector. The upper trough slightly deepened and a warm ridge ahead of the trough developed along the east coast. Due to the formation of the thermal ridge, the thermal advection increased. This warm ridge is a synoptic feature associated with the coastal development (Chen, 1954). Bosart (1981), in his investigation of the North American coastal cyclogenesis, pointed out that the mid-tropospheric short wave that propagates to the coast and the thermal ridge which develops in conjunction with the coastal front, provide a favourable environment for rapid cyclogenesis. The main difference between the case considered here and Bosart's is that the coastal front was enhanced in the lower troposphere in Bosart's case, but in the middle and upper troposphere in our one.

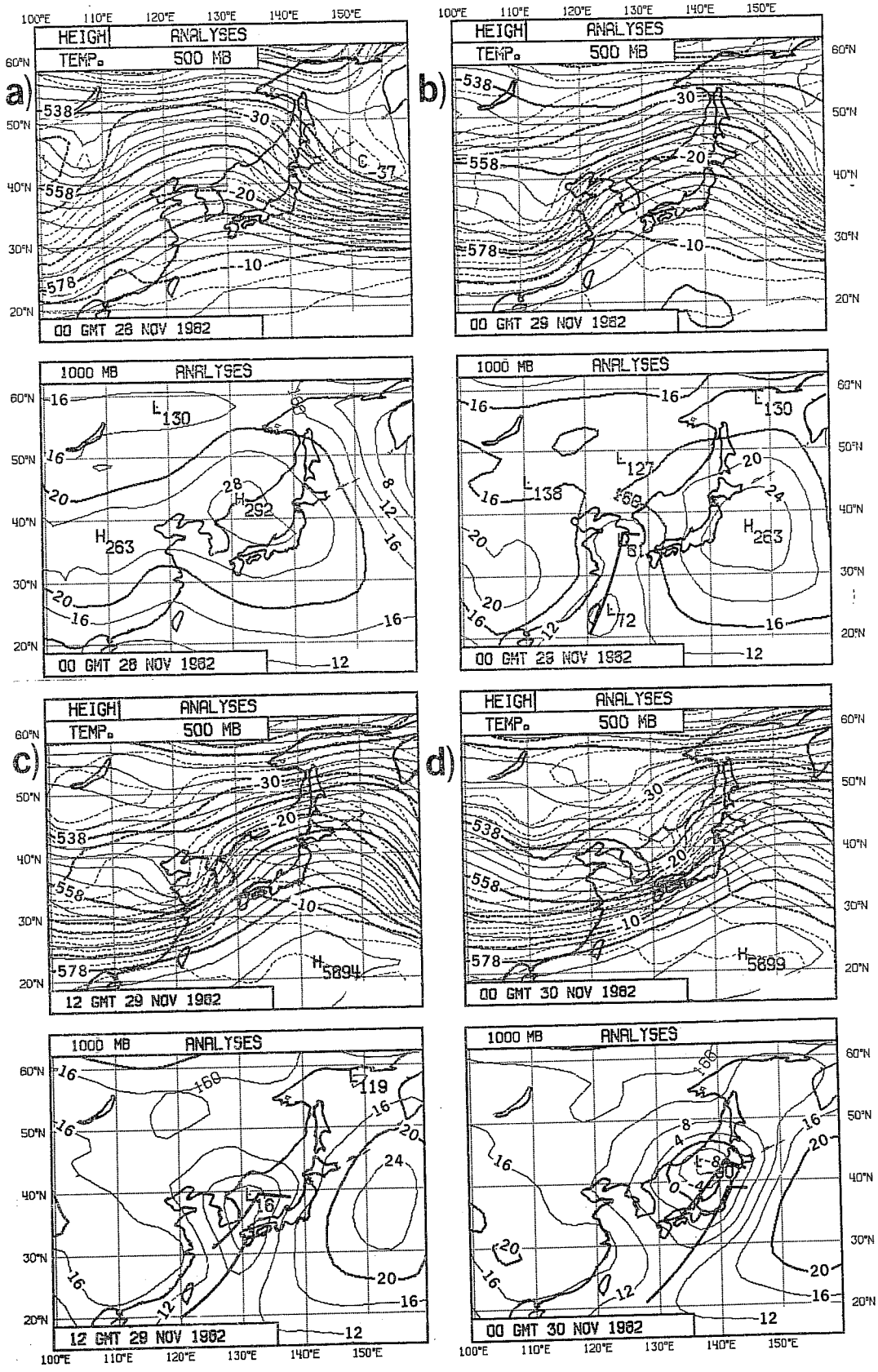

Fig. 1 ECMWF analyses at 500 mb and 1000 mb for (a) 00GMT 27 November 1982; (initial condition for the experiment), (b) 00GMT 28 November 1982, (c) 1200 GMT 29 November 1982, and (d) 00GMT 30 November 1982. Geopotential height contours (thin solid lines) every 40 m, temperature contours (dashed lines) every 2°C, surface fronts (thick lines) are from the analyses by Beijing Weather Centre.

The surface low moved northeastward, deepened markedly and reached a mature stage, with typical cold and warm fronts, by 12GMT 29 November. In the middle troposphere, the thermal ridge developed further and the warm advection over the surface warm front became more pronounced. By 00GMT 30 November, the cyclone moved over the Japanese Sea and became a major feature. The pressure dropped 21 mb within 24 h, i.e. nearly 1 mb per hour - the critical value suggested by Sanders and Gyakum (1980) to describe a "bomb". The upper trough then deepened with the further enhancement of the frontal zone and the thermal ridge. Both available potential energy and kinetic energy increased in the wave domain during this period, suggesting that the development was due to the internal diabatic processes rather than only to the adiabatic processes.

Uccellini et al. (1984), on the other hand, emphasised the role of the upper subtropical jet stream and the low level jet (LLJ) prior to the development. The upper level divergence in the entrance region, upstream and southward of a propagating jet maxima, could induce and strengthen the LLJ. The LLJ would then advect moisture and heat northward, thus contributing to the development of the thermal ridge. Fig. 2(a and b) shows the 200 mb and 700 mb wind field at 00GMT 29 November; an intense LLJ with maximum speed 27 m s^{-1} over South Korea at 700 mb and the 200 mb subtropical jet maxima with speed 80 m s^{-1} over north-east China are both apparent. The day before, the wind speed of the LLJ and subtropical jet were 15 m s^{-1} and 45 m s^{-1} respectively. Both the LLJ and subtropical jet were enhanced 24 h prior to the major development. The surface cyclone was on the cyclonic side of the LLJ and anticyclonic side of the subtropical jet - an area favourable for development since large upward motion is induced (Uccellini and Johnson, 1979).

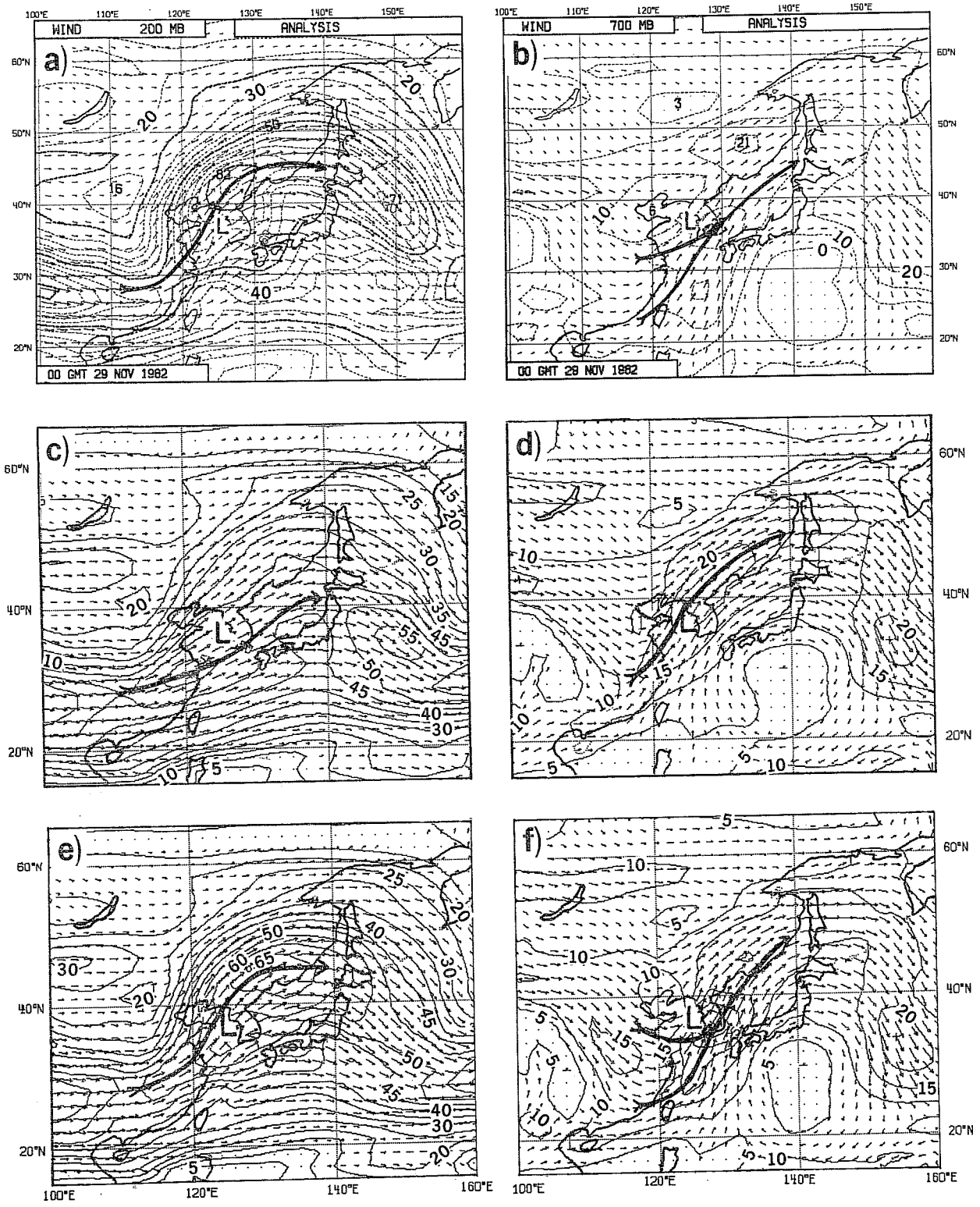

Fig. 2 (a) 200 mb and (b) 700 mb analysed wind field for 00GMT 28 November 1982; (c) and (d) same as in (a) and (b) but for the 24 h Dry simulation; (e) and (f) same as in (c) and (d) but for the Moist case. Dashed lines are isotach in m s $^{-1}$, arrow length proportional to the wind speed, thick lines denotes the jet, "L" denotes the location of the surface cyclonic circulation centre.

3. NUMERICAL RESULTS OF DRY AND MOIST SIMULATION

To investigate the impact of the latent heat release on the coastal cyclogenesis, two experiments were performed. One was a 48 h simulation without latent heat release due to condensation and convective activity, but moisture is still included in the model; here it will be called the 'Dry' simulation. The other was a 48 h 'Moist' simulation with latent heat release. The surface sensible heat flux is included in both experiments.

3.1 The Dry simulation

Fig. 3 shows the geopotential fields at 1000 and 500 mb from the 48 h Dry forecast that started at 00GMT 28 November 1982. The differences between forecast and analysis are remarkable. First, although some development is visible at 1000 mb, the major cyclone is not well predicted; its intensity is, in fact, much weaker than in the analysis. The cyclonic centre does not appear until after 48 h of integration, and its central pressure is 1008 mb against the analysed value of 987 mb. The forcing by the approaching upper trough initialised the cyclogenesis, but it is incapable of causing the cyclone to deepen rapidly.

Another apparent weakness in the Dry case is the model's inability to forecast the thermal ridge which developed ahead of the trough in conjunction with the enhancement of the front. The horizontal temperature gradient along the strong westerlies at 500 mb became weaker as the integration progressed; initially the gradient was about 1.7°C/100 km but decreased to 1°C/100 km after 48h. The conditions were more nearly equivalent barotropic in the Dry case and this caused reduced baroclinic development. On the other hand, the decrease of available potential energy means that the generation was insufficient in this case.

Finally, the Dry model did not forecast the strengthening of the LLJ and the subtropical jet prior to cyclone development - see (Fig. 2(c and d). The location of the LLJ was five hundred kilometres further north than in the analysis, and the jet maxima was over north-east China instead of South Korea. At 200 mb, the subtropical jet streak over north-east China was not predicted; the wind speed is 45 m s^{-1}, only about 56% of that in the analysis. The jet maximum moved to the lower Yangtze River at 30°N, about one thousand kilometres south of the actual location. The relative position of the surface low with respect to the LLJ and subtropical jet was reversed in the Dry case, i.e. the low was on the anticyclonic side of the LLJ and on the cyclonic side of the subtropical jet.

3.2 The Moist simulation

Fig. 4 shows the result of the Moist simulation. In contrast to the Dry case, the Moist model simulated the development of the cyclone successfully. The 24 hour forecast did predict the initial cyclogenesis off the coast, with the cyclonic circulation over the Yellow Sea correctly positioned, although the central pressure appeared slightly too low. In the 36 h and 48 h forecasts, the model simulated the rapid development. In fact, the forecast central pressure was nearly the same as the observed, and at 500 mb the development of the trough was also well predicted. Table 1 gives the observed and simulated central pressure of the cyclone for the two cases. The difference between the Dry and Moist cases increased with the duration of the forecasts: it was 11 mb at 24 h and 19 mb at 48 h, indicating the cumulative effect of the latent heat release.

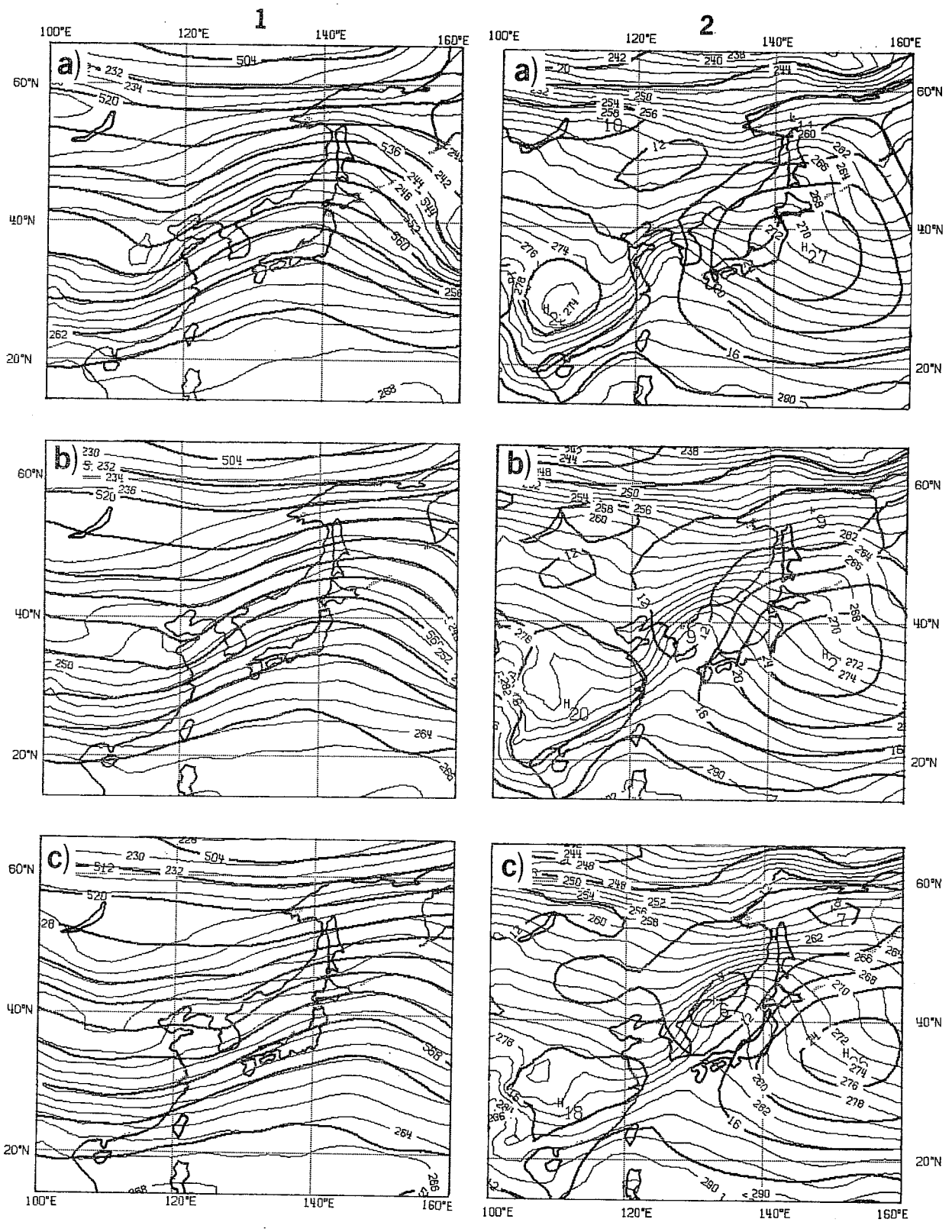

Fig. 3 Simulated (a) 24 h, (b) 36 h, (c) 48 h height and temperature at 500 mb (left) and 1000 mb (right) for Dry case, verifying with Fig. 1, (b), (c) and (d). Thick lines are geopotential height contours, unit in 10 m; thin lines are temperature contours, unit in K.

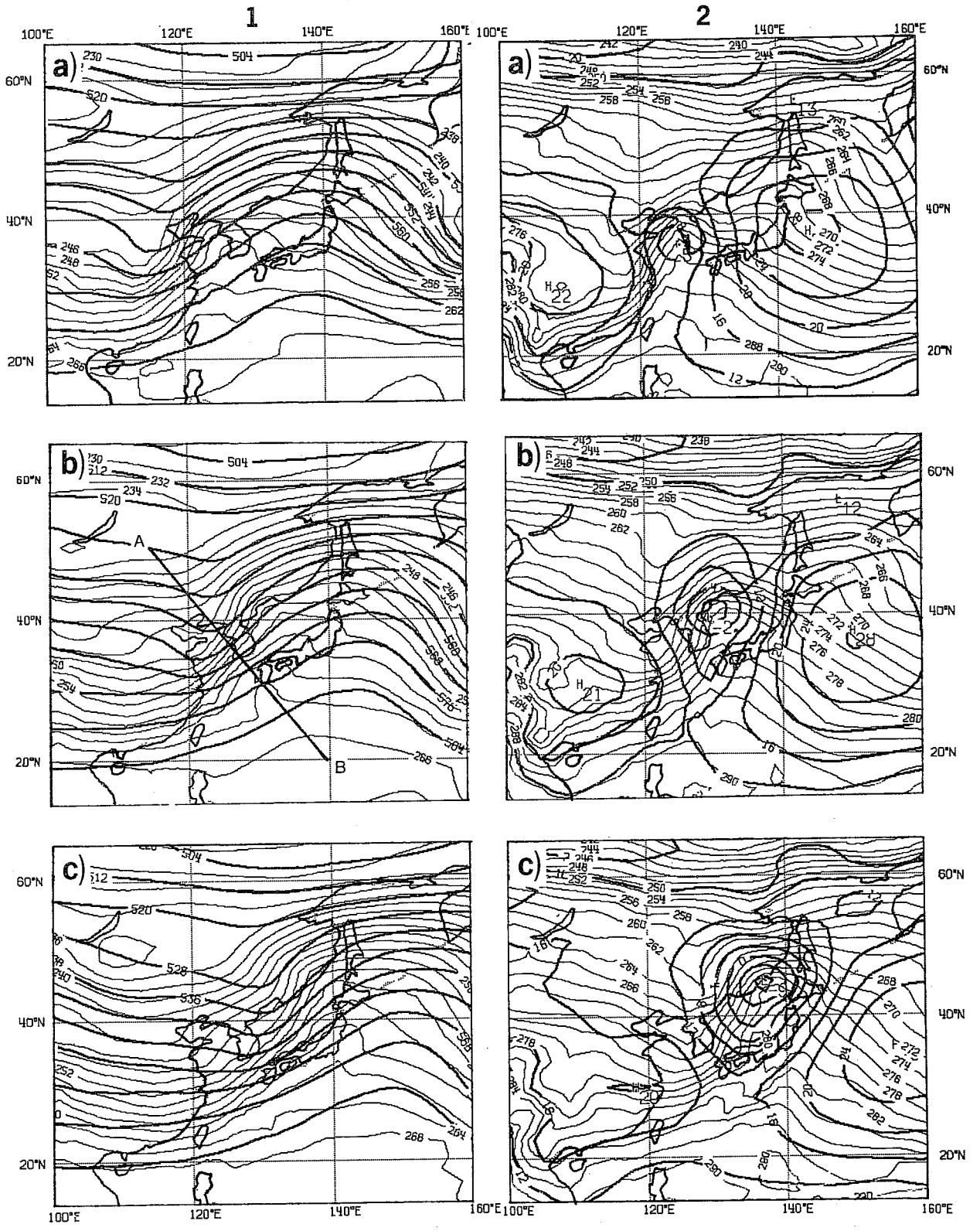

Fig. 4 Simulated (a) 24 h, (b) 36 h and (c) 48 h height and temperatures at 500 mb (left) and 1000 mb (right) for Moist case. Isolines are as in Fig. 3. Line AB in (b) is the path of vertical cross-section in Figs. 6 and 8.

Table 1 The observed and simulated central pressure of the cyclone (from 00GMT 28 November) every 12 h (in mb) in the Dry and Moist cases; "T" means trough.

	00h	12h	24h	36h	48h
Observed	1022(T)	1012	1008	997	987
Dry	1022(T)	1020(T)	1018(T)	1011	1008
Moist	1022(T)	1015(T)	1007	998	989

Another notable feature of the Moist case is the correct prediction of the enhancement of the thermal ridge and front. This can be illustrated by the difference of 500 mb temperature between the Moist and Dry cases (Fig. 5). In the first 24 h, temperature increased by 6°C in the area of the thermal ridge, while the change in the vicinity of the trough was nearly -2°C. At 48 h, the maximum change of the thermal ridge was up to 9.5°C. The predicted precipitation area was smaller than the area of warming; such warming is the response of the interaction between the dynamics and the latent heat release. Note the cooling near the trough reached less than $-4°C\ day^{-1}$ showing that the baroclinic instability was enhanced: the motion was no longer equivalent barotropic as in the Dry case. Such a process may be referred to as "latent heat feedback instability".

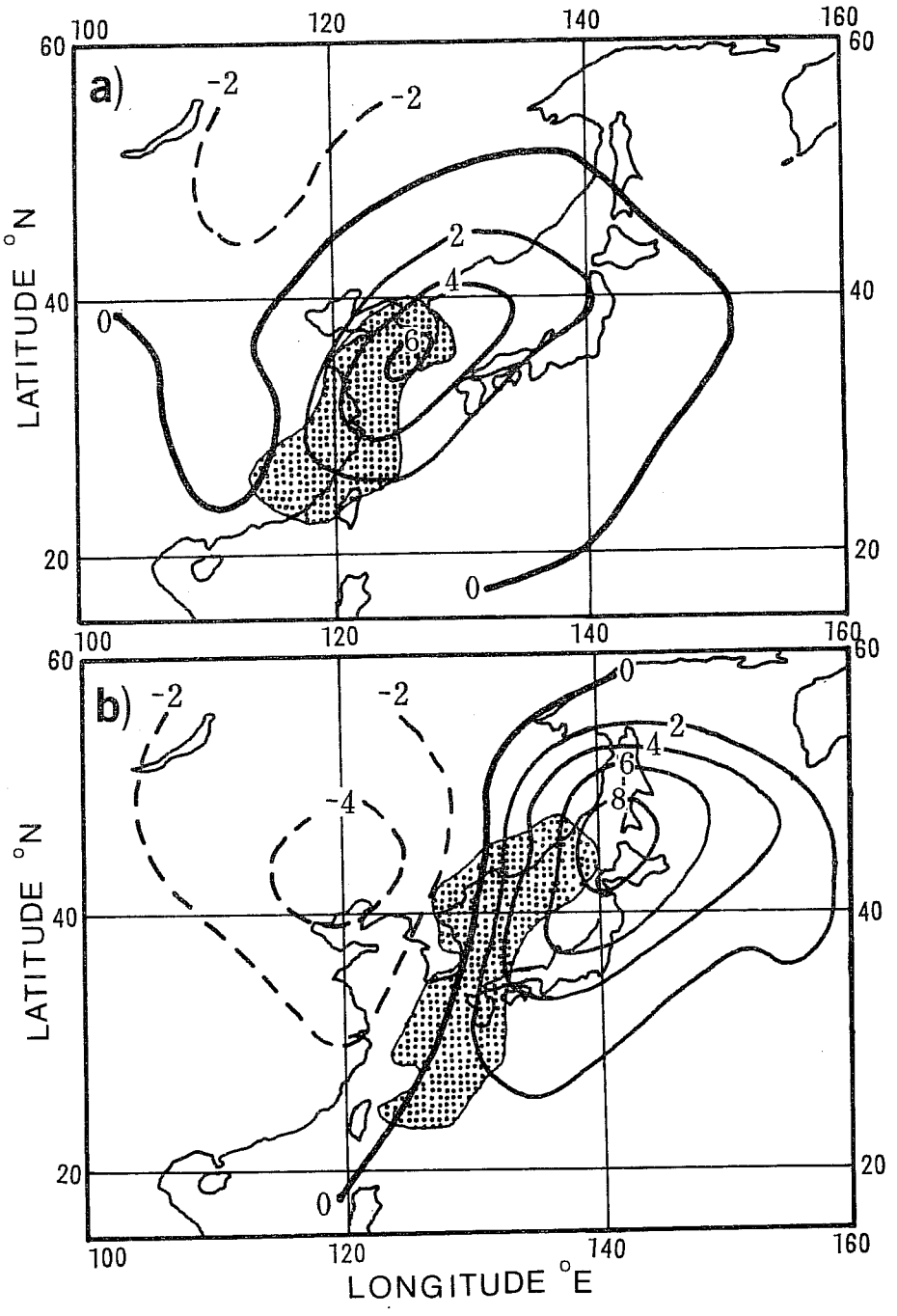

Fig. 5 Temperature difference at 500 mb for the Moist minus Dry case, (a) 24 h simulation, (b) 48 h simulation. Unit in °C; the stippled areas denote predicted 24 h precipitation greater than 10 mm day^{-1}.

4. IMPACT OF LATENT HEAT RELEASE ON THE BAROCLINIC WAVE

During winter, the fronts over East Asia and the Western Pacific are multi-structured; the upper subtropical front overlaps the polar front which appears as a deep baroclinic layer after a cold air outbreak (Hsieh, 1951; Mohri, 1953). For the present case, such features can be found in Fig. 6a which shows the observed meridional potential temperature gradient for the vertical cross-section (along the line AB indicated in Fig. 4b) for 12GMT 29 November 1982. Two large values of potential temperature gradient are evident; one extends from the surface to 600 mb and is associated with the polar front at 35°N, while the other lies above the polar front, extends from 600 mb to 250 mb and is associated with the subtropical front. Note there is a folded structure connected with the upper front. In the Dry case (Fig. 6b), the 36h simulated front below 600 mb appears with the correct intensity but is displaced compared with the analysis and the Moist case. The absence of moist processes does not affect the lower frontal structure very much, but does reduce its speed. Similar results were obtained by Baldwin et al. (1981) in their experiments with a two-dimensional model. The main differences between the Dry and Moist cases are in the middle and upper troposphere. In the Dry case the horizontal potential temperature gradient is not concentrated in a narrow band but appears as a broad baroclinic region, thus the upper subtropical front is absent. However in the Moist case (Fig. 6c) the gradient reaches 3.5°C/100 km within the subtropical front zone and the tropopause folding is comparable with that in the analysis. In general, the subtropical front and jet are maintained by the Hadley circulation (Palmen and Newton 1969), but in this case, the latent heat feedback process seems to be a contributing factor.

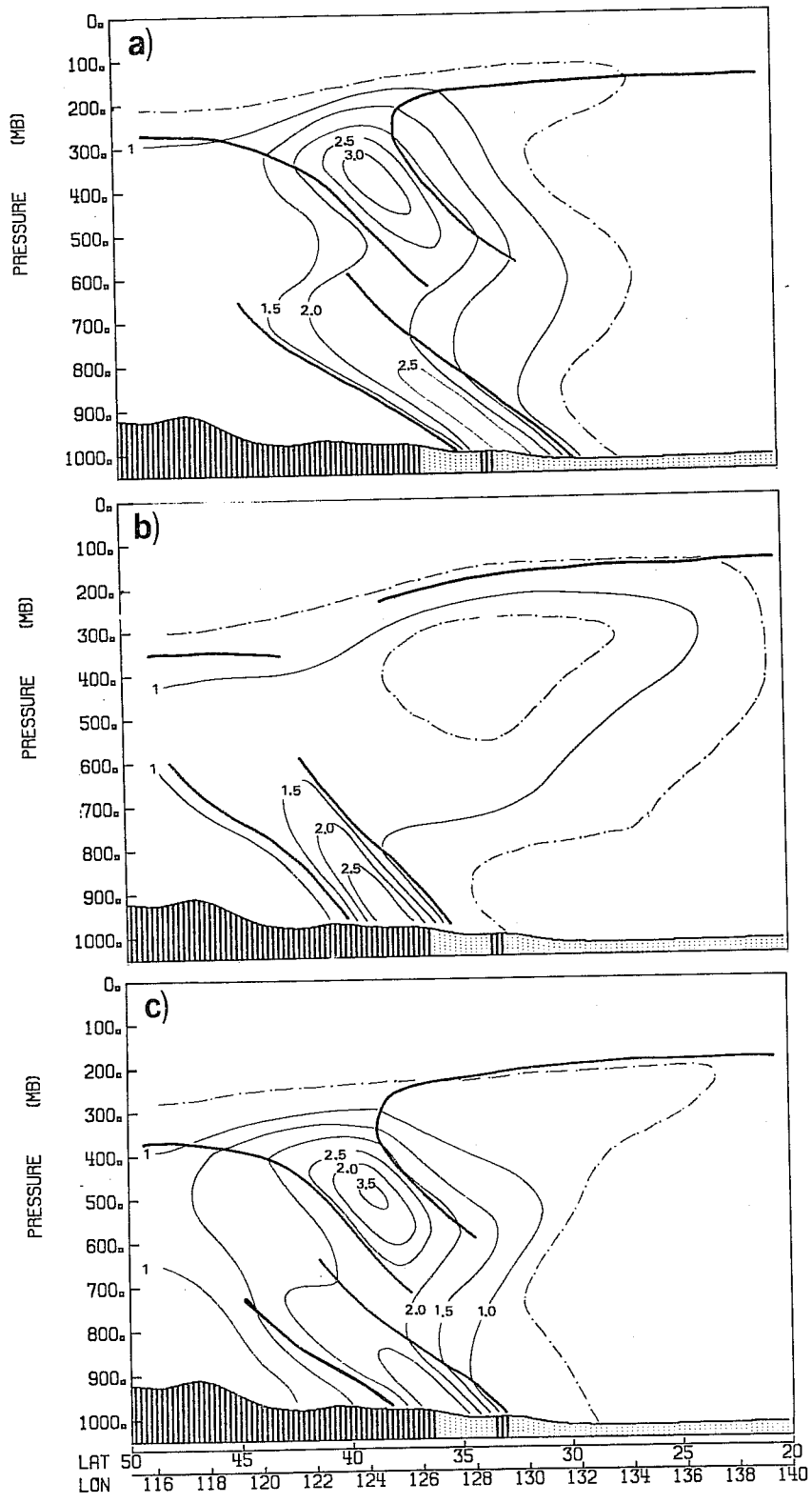

Fig. 6 Horizontal potential temperature gradient on the vertical cross section along line AB in Fig. 4(b): (a) verifying analysis for 12 GMT, 29 November, (b) same as in (a) but for the Dry 36 h simulation. (c) same as in (a) but for the Moist 36 h simulation. Unit is K/100 km; thick lines denote the frontal boundary and tropopause.

Fig. 7 shows the evolution of the vertical velocity field at 500 mb for the 24h and 48h forecast for both the Dry and Moist cases, and a comparison with the corresponding nephanalyses. The ascent in the frontal region for the Moist case (Fig. 7b) appears very active and is positioned over the area encompassing the major cloud system of the nephanalyses (Fig. 7c). At this level the Dry case has only a very weak vertical velocity (Fig. 7a), clearly showing that latent heat release is one of the determining factors of the subtropical front.

Fig. 8 presents the 36 h forecast for the ω field in the cross-section perpendicular to the front along the line AB of Fig. 4b. The diabatic heating due to the latent heat seems to intensify the magnitude and reduce the horizontal scale of upward motion in the warm air bounded by the front; the upward motion is enhanced to 1.6 pa s^{-1} in the moist experiment (Fig. 8a), about six times that in the day one (Fig. 8b). Also the upward motion is more concentrated in a narrow band, with the width of the upward motion zone being only 700 km in the Moist case but 1400 km in the Dry one. This is in agreement with the diagnostic results obtained by Krishnamurti (1968) and the numerical results of Baldwin et al. (1981). Due to the mass continuity, a subsidence with the large value of 0.2 pa s^{-1} occurred in the cold air north of the upward branch (39°N 124°E) which does not appear in the Dry case. The latent heat release in combination with the baroclinic process acts to produce a vertical direct circulation along the front which is more intense than with the simple baroclinic process, and it also produces a more intense indirect circulation in the war air. Such an induced vertical circulation is shown in Fig. 9. One branch of the circulation travels towards the north, subsides due to convergence and, as return flow in the cold air of the lower troposphere, moves southwards and converges near the surface. The other upper branch travels southwards and also subsides. This result confirms the scheme of the

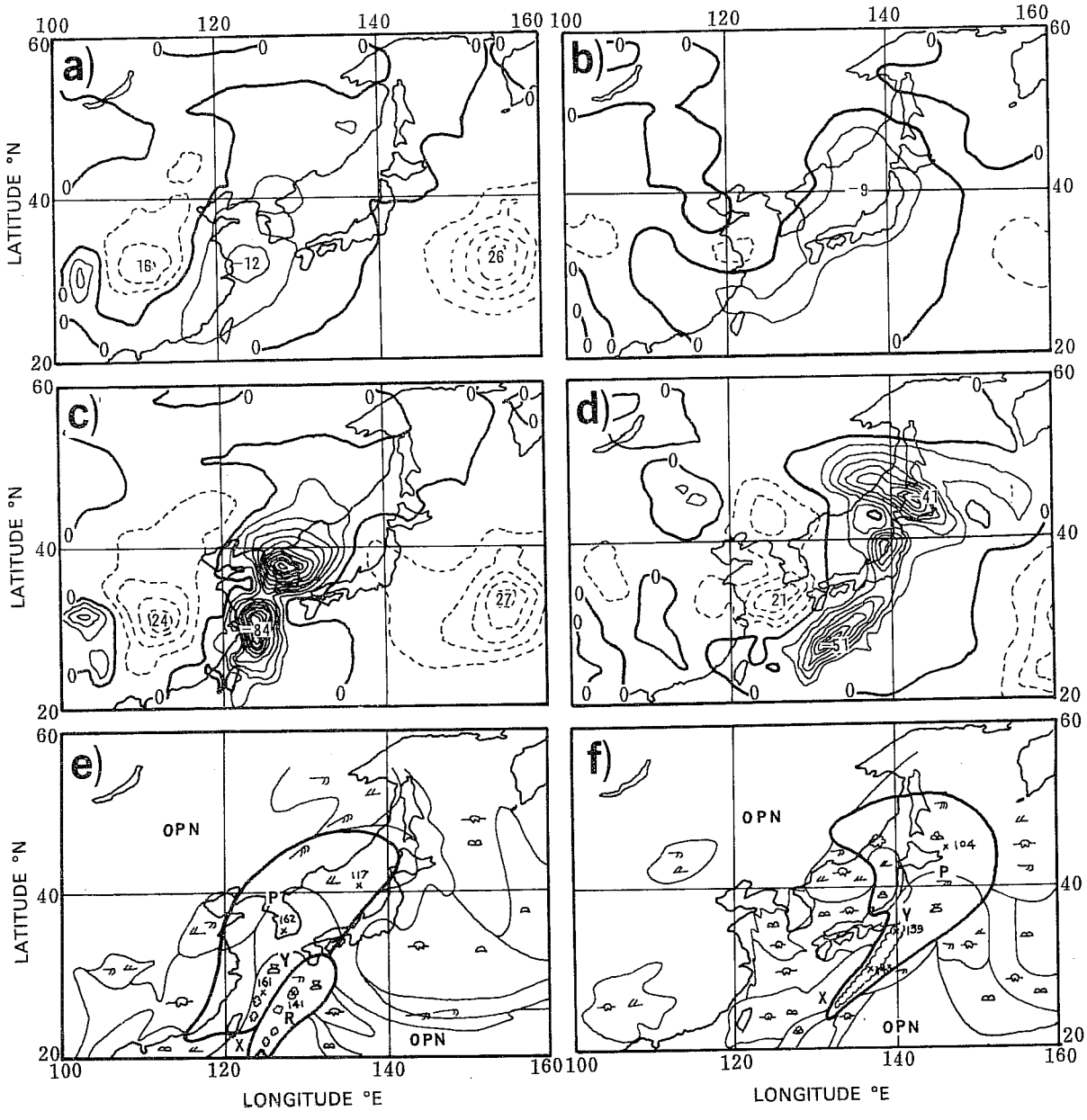

Fig. 7 Simulated (a) 24 h and (b) 48 h vertical velocity at 500 mb in Dry case; (c) and (d) same as in (a) and (b) but in Moist case. Contours every 5.10^{-2} P s^{-1}. The naphanalyses for (e) 00GMT 29 November 1982 and (f) 00GMT 30 November 1982, from the Monthly Report of the Meteorological Satellite Centre (1982). Thick lines mark the boundary of major cloud systems, indicated by X,Y,P,R. Scalloped lines denote active convective areas, OPN are open areas, the cross denotes the cloud height in 10^2 m.

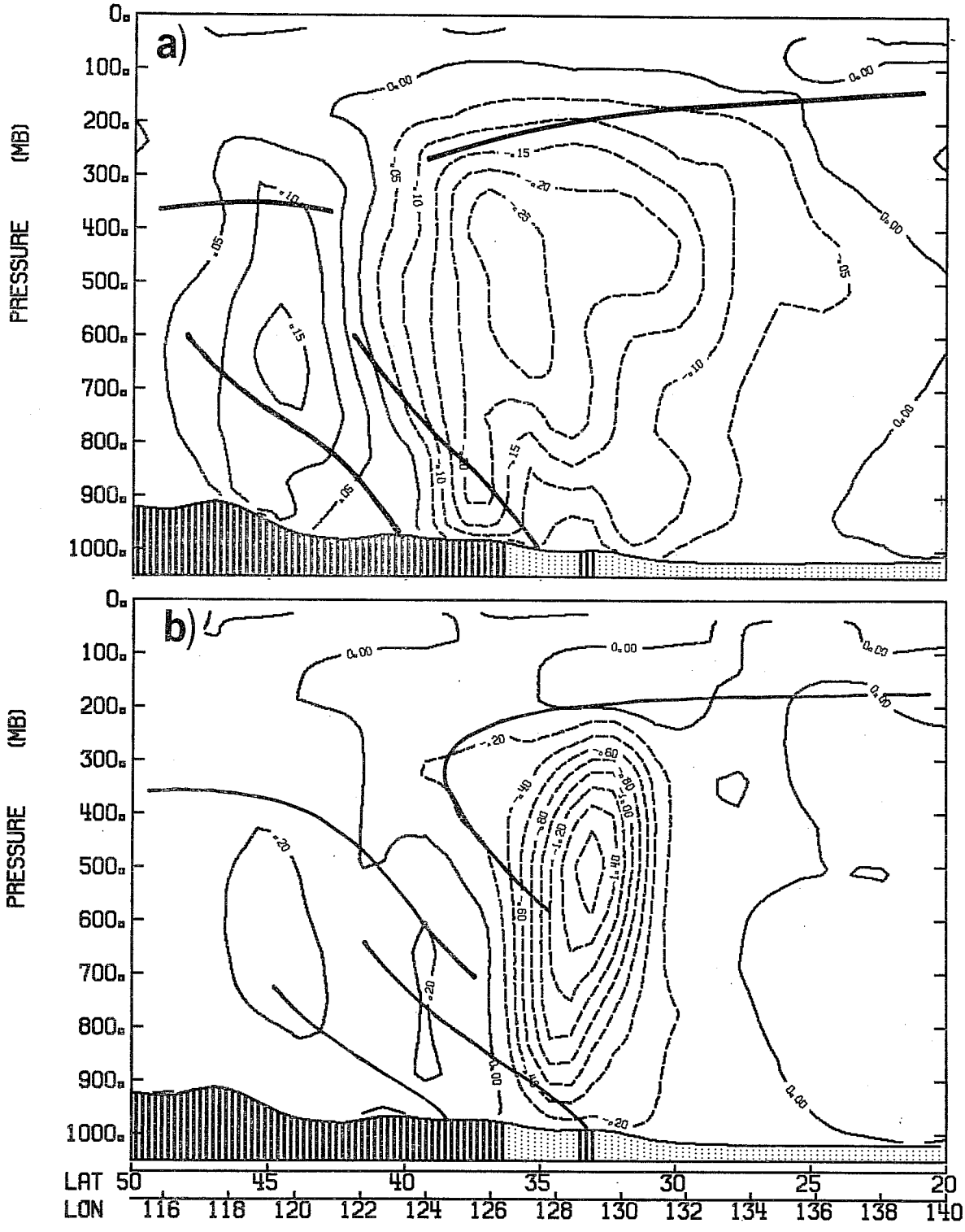

Fig. 8 Simulated 36 h vertical velocity on the cross-section along line AB in Fig. 4 (b). (a) Dry case, (b) Moist case. Unit is P s^{-1}; thick lines are the frontal boundary and tropopause.

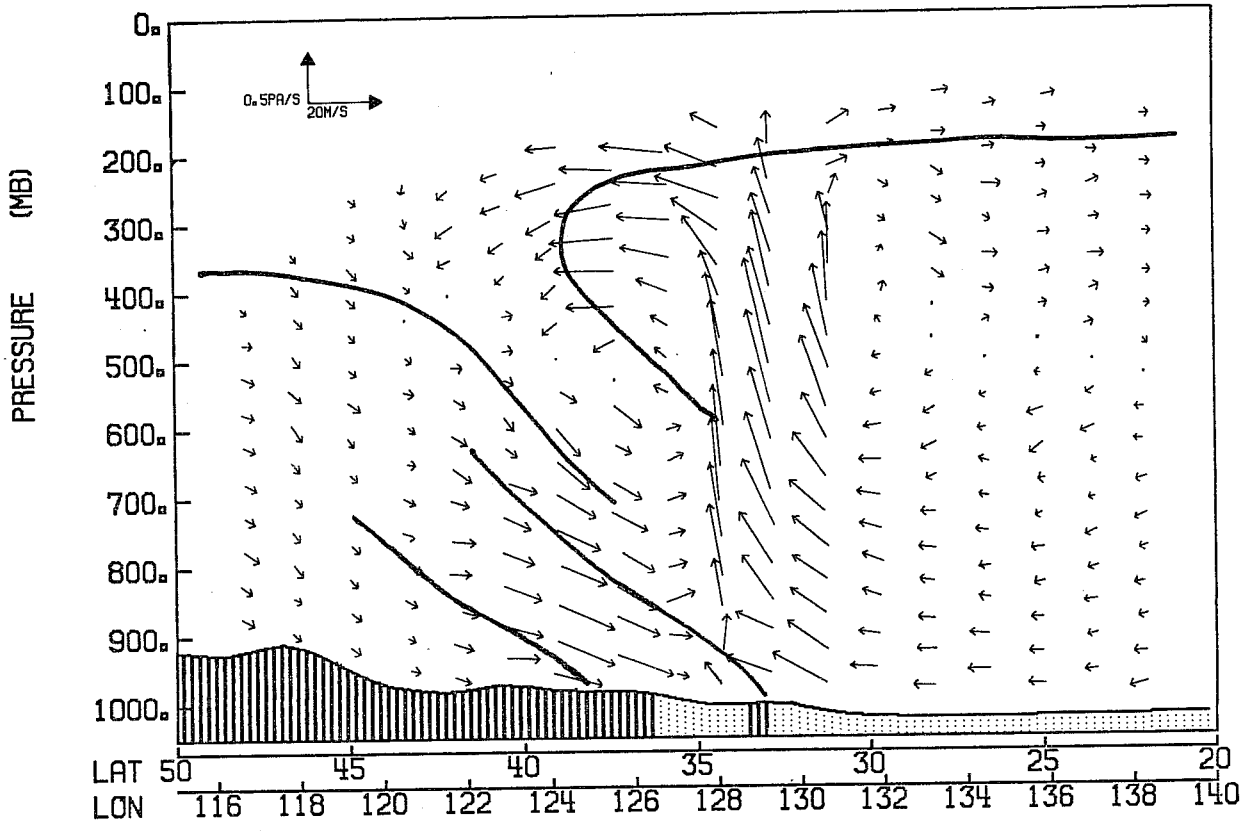

Fig. 9 The difference of 36 h simulated vertical transverse circulation for the cross-section as in Fig. 8 for the Moist case minus Dry case. Arrows are proportional to the speed (upper left corner); thick lines are the frontal boundary and tropopause in the Moist case.

circulation associated with a precipitating cloud system near a front discussed qualitatively by Palmen and Newton (1968, p.268). They also note that the upper convergence near the front is favourable to the frontogenesis.

In discussing the upper frontogenesis, Reed (1955) suggested that it is a thin slice of stratopheric air extruded into the mid-troposphere which causes the tropopause folding. Danielsen (1968) proposed a scheme for the vertical transverse circulation where direct and indirect cells, centred on the warm and cold air, form a confluence zone which is the region of upper frontogenesis and tropopause folding. In the Moist case, a direct circulation induced by the latent heat appears, but the indirect circulation in the cold air is absent. Nevertheless, a confluence zone along the upper front can be identified and the descent of the lower stratospheric air into the middle troposphere caused by the induced transverse circulation is evident.

The direct circulation along the front causes frontolysis due to the adiabatic cooling in the warm air, but if the latent heat release is taken into consideration, a warming takes place and causes frontogenesis in the conditionally unstable atmosphere. In a diagnostic study of frontogenesis, Rao (1966) also pointed out that the latent heating can cancel the adiabatic cooling and give rise to frontogenesis. On the other hand, the induced descent of stratospheric air into the mid-tropophere may be another effect causing frontogenesis (Reed, 1955). Uccellini et al. (1984) in analysing the Presidents Day coastal cyclone also noted the influence of tropopause folding on the rapid cyclone development similar to that found in this case.

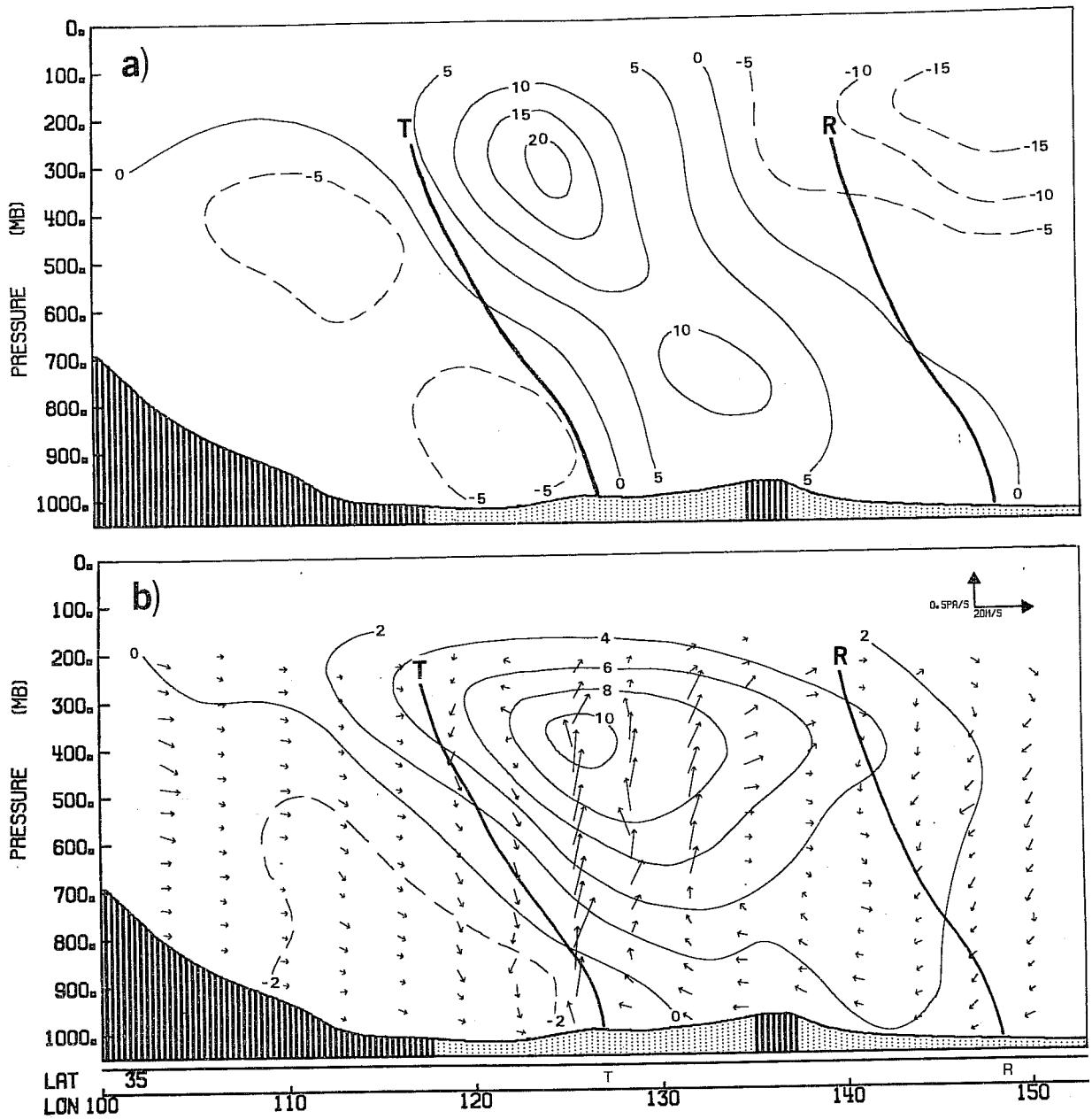

Fig. 10 The difference of 36 h simulated (a) northward wind velocity (m s^{-1}), (b) potential temperature (thin lines in K) and east-west over turning (arrows proportional to the speed) on the cross-section along 35°N relative to the trough line for the Moist minus Dry case. Thick lines denote trough (T) and ridge (R).

The change of the mid-tropospheric baroclinic wave due to the moist baroclinic process can be seen from Fig. 10, which shows the difference between the Moist and Dry 36 h forecast for the wind perpendicular to the cross-section (v), the potential temperature (θ) and the east-west turning of the wind along 35°N through the trough line. The change of v, indicating the change of the intensity of the disturbance, is asymmetric (Fig. 10a); compared to the Dry case the southerly wind ahead of the trough in the Moist case increases 10 m s^{-1} in the lower troposphere and up to 20 m s^{-1} in the upper troposphere, while the northerly wind behind the trough only increases by 5 m s^{-1}. The axis of maximum change tilts to the west following the axis of the trough, causing more angular momentum to be transported northward in the Moist case. A similar result was obtained by Chang et al. (1982) in a numerical study of North American cyclone development. Now consider the change in the θ field (Fig. 10b); a large area of warming ahead of the trough with maximum 10°C near 300 mb, and a small cooling (-2°C) behind, also shows an asymmetric structure. It is well known that the horizontal temperature gradient within a frontal zone is stronger on the east side of the trough than that on the west side in a well developed baroclinic wave (Palmen and Newton, 1969). Such a structure may be partly due to moist processes. The association of the warmer air with the strengthened southerly wind increases the northward transport of sensible heat, as well as the conversion of zonal available potential energy into eddy available potential energy. The difference of east-west over turning is also interesting - the increased ascent ahead of the trough divides into two branches in the upper troposphere; one turns to the west and descends behind the trough, while the other turns to the east and descends over the ridge region. The correlation between the changes of vertical velocity and θ indicates that the release of eddy available potential energy is increased in the vicinity of the wave, with the maximum ahead of the trough in the region of surface development.

5. ENERGY BUDGET

In sigma coordinates, the budget equations for the kinetic energy (KE) and sensible heat for a unit mass of air can be written in flux form (Savijärvi, 1983) as follows:

$$\frac{\partial}{\partial t}(p_s k) = -\nabla_\sigma(p_s k\underline{V}) - \frac{\partial}{\partial \sigma}(p_s k\dot{\sigma}) - p_s\underline{V}(\nabla_\sigma\phi + RT\nabla_\sigma \ln p_s) + p_s R_k$$

$$\frac{\partial}{\partial t}(p_s C_p T) = -\nabla_\sigma(p_s C_p T\underline{V}) - \frac{\partial}{\partial \sigma}(p_s C_p T\dot{\sigma}) + p_s \alpha\omega + p_s R_T$$

Here, p_s is the surface pressure, $k = \frac{1}{2}(u^2+v^2)$ the kinetic energy of horizontal flow, $\sigma = p/p_s$ the vertical coordinate, $u,v,\dot{\sigma} = d\sigma/dt$ the wind components, T and ϕ, the temperature and geopotential, $\alpha = RT/p$ the specific volume, $\omega = dp/dt$, and R_k and R_T are the residuals. In the KE budget equation, the term on the left hand side is the local change and the terms on the right hand side are the horizontal KE flux convergence, vertical KE flux convergence, KE generation and the residual. Physically, the residual is the KE dissipation through surface friction and internal friction. For the sensible heat budget equation, the term on the left hand side is the local change and the terms on the right hand side are the horizontal sensible heat flux convergence, vertical sensible heat flux convergence, adiabatic heating and the residual, which represents the diabatic heating sources. For a unit area column, the sensible heat is equivalent to the total potential energy (TPE) and so the adiabatic heating represents the release of TPE. If hydrostatic balance is assumed, the release of TPE and the generation of KE are linked through the geopotential flux convergence (Savijärvi, 1983):

$$-p_s\underline{V}\cdot(\nabla_\sigma\phi + RT\nabla_\sigma \ln p_s) = -\nabla_\sigma\cdot(p_s\phi\underline{V}) - \frac{\partial}{\partial\sigma}(p_s\phi\dot{\sigma} + \phi\sigma\frac{\partial p_s}{\partial t}) - p_s\alpha\omega$$

5.1 Kinetic energy budget

Fig. 11a shows the vertical ditribution of KE generation for both cases. Below 200 mb, the profiles have two maxima, one in the upper troposphere near 300 mb and the other near the surface in the planetary boundary layer; such features have been recognized by other investigator (e.g. Kung and Baker, 1975; Smith, 1980). Although the release of latent heat is dominant in the middle troposphere, the most significant KE differences are in the upper and lower troposphere. The enhancement of the KE generation in the upper troposphere is directly related to the increased ascent. Because the wind is stronger in the upper level, the ageostrophic wind is directed to the left of the isobaric contours, generating KE in the enhanced ascent area (Palmen and Newton, 1968, p.268). The secondary enhancement in the lower troposphere is the result of the cyclonic inflow toward the strengthened low system.
Fig. 11a also displays the vertical variation of the horizontal KE flux convergence. Due to the strengthened LLJ in the Moist case, which transports more KE into the domain, the horizontal KE flux convergence increases in the lower troposphere. In the upper troposphere, the increasing of the KE flux divergence is due to the subtropical jet north of the cyclone being stronger in the Moist case. On the whole the difference of the horizontal KE flux convergence between the two cases, as compared with the difference of KE generation, is less important in the KE budget.

5.2 Total potential energy budget

Table 3 shows the budget of sensible heat (total potential energy). It is evident that the TPE in the domain decreases in both cases, indicating a cooling rate of $-1.0°C\ day^{-1}$ in the Dry case and $-1.4°C\ day^{-1}$ in the Moist one. The tropospheric cooling is directly related to the adiabatic heating term (release of TPE) which is $-2.3°C\ day^{-1}$ and $-3.7°C\ day^{-1}$ in the Dry and

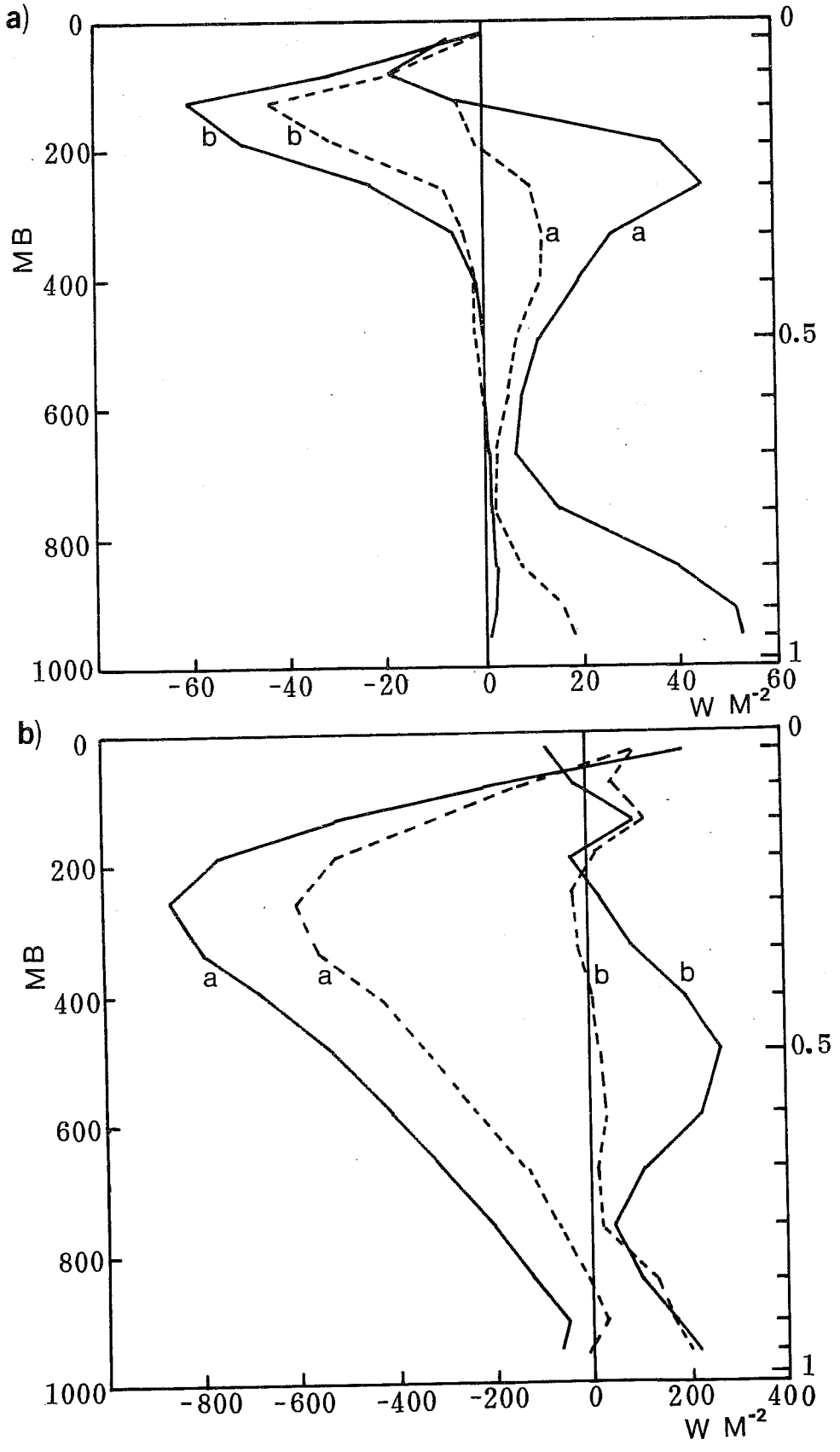

Fig. 11 (a) The vertical distribution of kinetic energy generation (curve a) and horizontal kinetic energy flux convergence (curve b) for the Dry (dashed lines) and Moist (solid lines) 24 h to 48 h simulation. (b) same as in (a), but for the adiabatic heating, i.e., total potential energy release (curve a) and diabatic heating (curve b).

Moist cases respectively. The remarkable increase of the TPE release is consistent with the latent heat induced vertical motion which is negatively correlated with α, as discussed in Sect.4. The maximum TPE release occurred at 250 mb (Fig. 11b) and its increase in the Moist experiment takes place over the whole troposphere. The enhanced conversion of TPE to KE is the dominant difference between the two TPE budgets.

Table 3. Area averaged vertically integrated total potential energy budget in the Dry and Moist simulations from 24 h to 48 h. Units in W m^{-2}, 115W m^{-1} ~ 1°C day^{-1}.

	$\frac{1}{g}\int_o^1 \frac{\partial[p_s C_p T]}{\partial t} d\sigma$	$\frac{-1}{g}\int_o^1 [\nabla_\sigma(p_s C_p \underline{TV})] d\sigma$	$p_s \alpha\omega$	$p_s R_T$
Dry	-114	110	-267	43
Moist	-163	132	-422	127

On the other hand, an increase in diabatic heating of 0.7°C day^{-1} in the Moist case is also noticeable. Fig. 11b displays the vertical distribution of the diabatic heating. There is no difference below 800 mb; this mean that the surface sensible heat fluxes which cause the lower tropospheric heating are the same in both cases. The maximum heating of 2.2°C day^{-1} which occurs at 500 mb in the Moist case is absent in the Dry case and this shows the impact of latent heat release. Compared with the adiabatic heating, the direct latent heat induced TPE changes are not efficient in the TPE budget. Rather, the dynamic response to the latent heat (i.e. the adiabatic heating) is the main process which enhances the conversion from potential to kinetic energy within the cyclone.

6. SUMMARY AND CONCLUSION

A typical major cyclone development off the East Asian coast was studied by performing numerical simulations. Results from an experiment using a model without latent heat release (Dry) shows that the baroclinic forcing of the initial development of the cyclone was produced when the middle tropospheric short wave approached the inverted surface trough. However, only a shallow cyclone was produced. Thus we can assume that the dry baroclinic process can not be the cause of the rapid cyclogenesis. In the experiment with the model with the moist processes included, the rapid development was predicted.

The cyclone developed remarkably and reached the same intensity as that in the analysis. From this it may be inferred that the main mechanism for the development of the East Asia coastal cyclone is the moist baroclinic process (Hsieh, 1979).

By comparing the Moist case with the Dry case we can deduce that:

(a) The latent heat feedback process not only enhances the vertical motion in the precipitation area, but also causes subtropical frontogenesis in the upper troposphere and intensifies the thermal ridge east of the trough. The development of the thermal ridge, which accompanied the increase of the thermal advection, is substantial when cyclogenesis occurs.

(b) The strengthening of the upper subtropical jet stream and the lower level jet, which creates a favourable environment for the development, is mainly caused by the dynamic response to the latent heating.

(c) The asymmetric distribution of the wind and temperature in the baroclinic wave is more pronounced in the Moist case. Therefore the northward transport of sensible heat and angular momentum, as well as the conversion of zonal available potential energy to the eddy available potential energy and the gain of kinetic energy, are increased.

The present study and other numerical investigations (Hoskins, 1980; Chen et al. 1983) showed that the role of release of latent heat in the strengthening of the frontal transition zone, the vertical velocity and the baroclinic instability are by no means negligible for some kinds of coastal and oceanic cyclones where the moisture supply is sufficient. Of course, further cases studied are needed to clarify this result because the latent feedback process is very complicated in cyclones.

References

Aubert, E.J., 1957: On the release of latent heat as a factor in large scale atmospheric motions. J.Meteor. 14, 527-542.

Baldwin, D.G., E.-Y. Hsie, R.A. Anthes and D. Keyser, 1981: A numerical study of the influence of the planetary boundary layer and moisture on frontal structure. Amer.Meteor.Soc., Fifth Conference on Numerical Weather Prediction, Nov.2-6, 1981 Monterey, Ca., 191-197.

Bosart, L.F., 1981: The Presidents' Day snowstorm of 18-19 February 1979: A subsynoptic-scale event. Mon.Wea.Rev., 109, 1542-1566.

Bjerknes, J., 1919: On the structure of moving cyclones. Geofys.Publ., 1, No.2, 8pp.

Burridge, D.M. and J. Haseler, 1977: A model for medium range weather forecasts - adiabatic formulation. ECMWF Tech.Rep.No.4, 46pp.

Chang, C.B., D.J. Perkey and C.W. Kreitzberg, 1982: A numerical case study of the effects of latent heating on a developing wave cyclone. J.Atmos.Sci., 39, 1555-1570.

Chang, C.B., D.J. Perkey and C.W. Kreitzberg, 1984: Latent heat induced energy transformations during cyclogenesis. Mon.Wea.Rev., 112, 357-367.

Charney, J.G., 1947: The dynamics of long waves in a baroclinic westerly current. J.Meteor., 4, 135-162.

Chen, H.Y., 1954: Two case study of the developmnt of the cyclone over East Sea. Acta Meteor.Sinica, 25, 213-231.

Chen, T.-C., C.-B. Chang and D.J. Perkey, 1983: Numerical study of an AMTEX '75 oceanic cyclone. Mon.Wea.Rev., 111, 1818-1829.

Danard, M.B., 1964: On the influence of released latent heat on cyclone development. J.Appl.Meteor., 3, 27-37.

Danielsen, E.F., 1968: Stratospheric-tropospheric exchange based on radioactivity, ozone and potential vorticity. J.Atmos.Sci., 25, 502-518.

Eady, E.T., 1949: Long wave and cyclone waves. Tellus, 1, 33-52.

Edmon, H.J., Jr., 1978: A reexamination of limited-area available potential energy budget equations. J.Atmos.Sci., 35, 1655-1659.

Eliassen, A., 1966: Motions of intermediate scale: Fronts and cyclones. Advance in Earth Science, MIT Press, 111-138.

Holton, J.R., 1979: An Introduction to Dynamic Meteorology, Academic Press. 2nd. ed. International geophysics series, Vol.23. New York, 391pp.

Hoskins, B.J., 1980: Effect of diabatic processes on transient mid-latitude waves. ECMWF Workshop on Diagnostics of Diabatic Processes, 23-25 April 1980, 85-99.

Hsieh, Y.P., 1951: On the wind and temperature fields over Pacific and Eastern Asia in winter. J.Chinese Geophys.Soc., 2, 279-288.

Hsieh, Y.P., 1979: Dynamics of the moist baroclinic atmosphere. Collected Papers on Heavy Rainstorm. 1-15.

Kung, E.C. and P.J. Smith, 1974: Problems of large-scale kinetic energy balance. A diagnostic analysis in GARP. Bull.Amer.Meteor.Soc., 55, 768-777.

Kung, E.C. and W.E. Baker, 1975: Energy transformations in the middle-latitude disturbances. Quart.J.Roy.Meteor.Soc., 101, 793-815.

Kuo, H.L., 1974: Further studies of the parameterization of the influence of cumulus convection on large-scale flow. J.Atmos.Sci., 31, 1232-1240.

Kutzbach, G., 1979: The thermal theory of cyclones: A history of meteorological thought in the nineteenth century. Historical Monograph Series, Amer.Meteor.Soc., 255p.

Monthly Report of Meteorological Satellite Centre, Nov. 1982, Meteorological Satellite Centre, Tokyo, Japan.

Mohri, K., 1953: On the fields of wind and temperature over Japan and adjacent waters during winter of 1950-1951. Tellus, 5, 340-358.

Palmen, E. and C.W. Newton, 1969: Atmospheric Circulation Systems. Their structure and physical interpolation. International Geophysics Series, Vol.13. Academic Press, 603pp.

Petterssen, S., 1956: Weather Analysis and Forecasting, 2nd ed. Vol.1. McGraw-Hill, New York, 428pp.

Rao, G.V., 1966: On the influences of fields of motion, baroclinicity and latent heat source on frontogenesis. J.Appl.Meteor., 5, 377-387.

Reed, R.J., 1955: A study of a characteristic type of upper-level frontogenesis. J.Meteor., 12, 226-237.

Sanders, F. and J.R. Gyakum, 1980: Synoptic-dynamic climatology of the "bomb". Mon.Wea.Rev., 108, 1589-1606.

Savijärvi, H., 1983: The atmospheric energy budgets over North America, the North Atlantic and Europe based on ECMWF analyses and forecasts. Tellus, 35A, 39-50.

Smith, P.J., 1980: The energetics of extratropical cyclones. Rev. Geophys. Space Phy., 18, 378-386.

Staff Members Academia Sinica, 1958: On the general circulation over Eastern Asia (II). Tellus, 10, 58-75.

Tiedtke, M., J.-F. Geleyn, A. Hollingsworth, and J.-F. Louis, 1979: ECMWF model, parameterization of subgrid scale processes. ECMWF Tech.Rep.No.10, 45pp.

Uccellini, L.W. and D.R. Johnson, 1978: The coupling of upper- and lower-tropospheric jet streaks and implications for the development of severe convective storms. Mon.Wea.Rev., 107, 682-703.

Uccellini, L.W., P.J. Kocin, R.A. Petersen, C.H. Wash and K.F. Brill, 1984: The presidents' day cyclone 18-19 February 1979: Synoptic overview and analysis of the subtropical jet streak influencing the pre-cyclogenetic period. Mon.Wea.Rev., 112, 31-55.

ECMWF PUBLISHED TECHNICAL REPORTS

No.1 A Case Study of a Ten Day Prediction

No.2 The Effect of Arithmetic Precisions on some Meteorological Integrations

No.3 Mixed-Radix Fast Fourier Transforms without Reordering

No.4 A Model for Medium-Range Weather Forecasting - Adiabatic Formulation

No.5 A Study of some Parameterizations of Sub-Grid Processes in a Baroclinic Wave in a Two-Dimensional Model

No.6 The ECMWF Analysis and Data Assimilation Scheme - Analysis of Mass and Wind Fields

No.7 A Ten Day High Resolution Non-Adiabatic Spectral Integration: A Comparative Study

No.8 On the Asymptotic Behaviour of Simple Stochastic-Dynamic Systems

No.9 On Balance Requirements as Initial Conditions

No.10 ECMWF Model - Parameterization of Sub-Grid Processes

No.11 Normal Mode Initialization for a Multi-Level Gridpoint Model

No.12 Data Assimilation Experiments

No.13 Comparisons of Medium Range Forecasts made with two Parameterization Schemes

No.14 On Initial Conditions for Non-Hydrostatic Models

No.15 Adiabatic Formulation and Organization of ECMWF's Spectral Model

No.16 Model Studies of a Developing Boundary Layer over the Ocean

No.17 The Response of a Global Barotropic Model to Forcing by Large-Scale Orography

No.18 Confidence Limits for Verification and Energetic Studies

No.19 A Low Order Barotropic Model on the Sphere with the Orographic and Newtonian Forcing

No.20 A Review of the Normal Mode Initialization Method

No.21 The Adjoint Equation Technique Applied to Meteorological Problems

No.22 The Use of Empirical Methods for Mesoscale Pressure Forecasts

No.23 Comparison of Medium Range Forecasts made with Models using Spectral or Finite Difference Techniques in the Horizontal

No.24 On the Average Errors of an Ensemble of Forecasts

ECMWF PUBLISHED TECHNICAL REPORTS

No.25 On the Atmospheric Factors Affecting the Levantine Sea

No.26 Tropical Influences on Stationary Wave Motion in Middle and High Latitudes

No.27 The Energy Budgets in North America, North Atlantic and Europe Based on ECMWF Analyses and Forecasts

No.28 An Energy and Angular-Momentum Conserving Vertical Finite-Difference Scheme, Hybrid Coordinates, and Medium-Range Weather Prediction

No.29 Orographic Influences on Mediterranean Lee Cyclogenesis and European Blocking in a Global Numerical Model

No.30 Review and Re-assessment of ECNET - a Private Network with Open Architecture

No.31 An Investigation of the Impact at Middle and High Latitudes of Tropical Forecast Errors

No.32 Short and Medium Range Forecast Differences between a Spectral and Grid Point Model. An Extensive Quasi-Operational Comparison

No.33 Numerical Simulations of a Case of Blocking: the Effects of Orography and Land-Sea Contrast

No.34 The Impact of Cloud Track Wind Data on Global Analyses and Medium Range Forecasts

No.35 Energy Budget Calculations at ECMWF: Part I: Analyses

No.36 Operational Verification of ECMWF Forecast Fields and Results for 1980-1981

No.37 High Resolution Experiments with the ECMWF Model: a Case Study

No.38 The Response of the ECMWF Global Model to the El-Nino Anomaly in Extended Range Prediction Experiments

No.39 On the Parameterization of Vertical Diffusion in Large-Scale Atmospheric Models

No.40 Spectral characteristics of the ECMWF Objective Analysis System

No.41 Systematic Errors in the Baroclinic Waves of the ECMWF Model

No.42 On Long Stationary and Transient Atmospheric Waves

No.43 A New Convective Adjustment Scheme

No.44 Numerical Experiments on the Simulation of the 1979 Asian Summer Monsoon

No.45 The Effect of Mechanical Forcing on the Formation of a Mesoscale Vortex

ECMWF PUBLISHED TECHNICAL REPORTS

No.46 Cloud Prediction in the ECMWF Model

No.47 Impact of Aircraft Wind Data on ECMWF Analyses and Forecasts during the FGGE Period, 8-19 November 1979 (not on WP, text provided by Baede)

No.48 A Numerical Case Study of East Asian Coastal Cyclogenesis